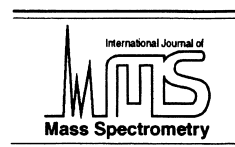




ELSEVIER

International Journal of Mass Spectrometry 209 (2001) 5–21



Speciation of chromium compounds by laser ablation/ionization mass spectrometry and a study of matrix effects

Frédéric Aubriet*, Benoît Maunit, Jean-François Muller*

Laboratoire de Spectrométrie de Masse et de Chimie Laser, IPEM, Université de Metz, 1, Boulevard Arago 57078 Metz, Cedex 03, France

Received 7 July 2000; accepted 31 October 2000

Abstract

The capabilities of the laser ablation/ionization technique coupled to a Fourier transform ion cyclotron resonance mass spectrometer for the speciation of chromium compounds were evaluated and various analytical processes have been investigated. A better knowledge of the pathways of cluster ion formation allows us to propose a simple and reliable methodology for the identification of the chromium chemical state. In the negative ion mode, the Cr_xO_y^- ions are generated by aggregative processes between CrO_2^- or CrO_3^- ions on the one hand and CrO_2 and/or CrO_3 neutrals on the other. The more oxygenated species are produced during the laser ablation of hexavalent chromium compounds. In addition, hydrogenated ions are formed in the study of hydrated trivalent chromium compounds. The choice of only two ion intensity ratios allows to distinguish unambiguously trivalent, hydrated trivalent, and hexavalent chromium compounds, respectively. This new methodology, based on the examination of nearly 20 chromium reference compounds, was evaluated in the study of simple system (pure chromium compounds and commercial pigment). The influence of various oxides, which are generally present in polyphasic and complex matrices, on the methodology proposed is finally evaluated. An antagonistic effect between first calcium and silicon oxides and second trivalent iron and zinc oxides is observed and allows to indicate the limitations of the method. It was demonstrated that the introduction of this kind of oxide induces important modifications in the distribution of the species in the gas cloud after the laser ablation and consequently in the processes of cluster ion formation. Silicon and lime involved competitive reaction with chromium species and lead to less oxygenated Cr_xO_y^- ions whereas zincite and hematite assisted the formation of highly oxygenated chromium species. (Int J Mass Spectrom 209 (2001) 5–21) © 2001 Elsevier Science B.V.

Keywords: Inorganic mass spectrometry; Chromium speciation; FTICRMS; Aggregation processes; Matrix effects

1. Introduction

Due to its significance from a health point of view, the speciation of mineral compounds is actually an important field of investigation. However, the classi-

cal “liquid techniques” seem often to be quite limited, especially when solubilization and/or preconcentration steps are needed prior to the study of a sample. This is the reason why “solid techniques,” i.e. in situ techniques like x-ray diffraction, Raman spectroscopy, or mass spectrometry are used to overcome the problem of metal chemical state alteration during pretreatment steps. In this context, the use of mass spectrometric techniques in the differentiation of the

* Corresponding authors.

E-mail addresses: jfmuller@ismcl.sciences.univ-metz.fr; aubriet@ismcl.sciences.univ-metz.fr

valence number and more generally in the speciation of mineral compounds is relatively recent. Most often used techniques are the static secondary ions mass spectrometry sSIMS [1], the laser ablation mass spectrometry [2–4], and the electrospray ionization mass spectrometry ESIMS [5–8].

The speciation of inorganic compounds is generally carried out for environmental reasons [9,10]—the toxicity of a mineral compound is indeed, in many cases dependent on its chemical state, to follow-up the synthesis of thin films [11,12] or to study corrosion processes [13]. Speciation may also be powerful in the study catalyst modifications [14] or to follow the evolution of mineral compounds in cellular medium [15–18]. Finally, mass spectrometry techniques are equally used to distinguish two samples of a same compound synthesized according to different experimental methods [19].

In the field of chromium chemical state speciation some articles have already been published. By considering the distribution of the negative cluster ions observed in the mass spectra of reference compounds at the 266 nm wavelength, our laboratory [20–22] proposed a methodology based on time-of-flight-laser microprobe mass spectrometry (TOF-LMMS) experiments for the differentiation of trivalent, hydrated trivalent and hexavalent chromium compounds. This method is well adapted to the analysis of particles and was applied to the examination of complex industrial dust particles and biological matrices [20,23]. By using the same kind of speciation criteria, Poels et al. [24] proposed an alternative method to distinguish trivalent and hexavalent chromium oxides by Fourier transform ion cyclotron resonance mass spectrometry (FTICRMS) ($\lambda = 266$ nm). By applying rapid single particle mass spectrometry to the speciation of chromium, Neubauer et al. [25] obtained in the negative ion mode of detection criteria of differentiation for trivalent and hexavalent chromium compounds comparable to those proposed earlier by Poitevin and co-workers [20–23]. A discriminating quadratic analysis also allows them to classify successfully the results obtained in the examination of mixtures of trivalent and hexavalent chromium compounds.

Stewart and Horlick [6] investigated the influence

of several instrumental and experimental parameters on the distribution of chromium species in solution by ESIMS. Gwizdala et al. [26] proposed an ESIMS methodology for the differentiation of the valence number +III and +VI of chromium by considering specific ions. Although the method of Gwizdala et al. appears powerful and simple, it has the same drawback that other methods often used in the liquid phase. The solid phase methods are consequently more adapted to account for the distribution of the species of chromium in the sample studied, even if the achievement of quantitative or at least semiquantitative information is more delicate. For this reason, the method developed by Poitevin and co-workers [20–23] seems to be a powerful alternative. However this method which allows an analysis particle by particle cannot lead to a global information. Further, this methodology was established with only a few reference compounds: trivalent and hexavalent chromium oxides; sodium, potassium, and calcium chromates; hydrated trivalent chromium nitrate and sulfate. Although these results constitute a notable improvement of previous studies, the great part of the speciation methods by mass spectrometry consist only in the examination of oxides, it may however seem limited. Moreover, the protocol of differentiation [20] is relatively complex and may sometimes involve a difficulty in the final diagnostic. To improve this methodology, we will describe here our investigations with the LA-FTICRMS microprobe. By tripling the number of reference compounds, we tried to establish a less complex and more accurate methodology of speciation. Further, the use of our FTICRMS microprobe allows to tune the diameter of the laser spot with its focusing/defocusing telescope. For example, with a power density of 5×10^7 W/cm², the spot diameter is 400 μ m.

Further, other speciation methodologies carried out for distinguishing oxides or salts of transition or post transition metals have been proposed and are generally based on: (1) the methodology established by Plog (see sec. 2); (2) the calculations of intensity ratios, or (3) the presence of specific and characteristic ions.

The transposition of the Plog model to the study of titanium oxides by TOF-LMMS allowed Michiels and Gijbels [2] to discriminate them in the both mode of detection. A similar study done by Lobstein et al. [11] corroborated these results and allowed control of the stoichiometry of anatase (TiO_2) thin films synthesized by pulsed laser deposition on polyethylene terephthalate substrates. In fact, the successful application of Plog model depends on a greater formation of highly oxygenated ions for oxides including the transition metal in a greater oxidation state. Consequently, the study of the ion distribution with different oxygen/metal ratios often constituted relevant speciation criteria such as in the study of molybdenum [27], iron [27–30], lead [9], or arsenic [10] oxides. In this latter study the distribution of As_3O_x^- ions is used to carry out semiquantitative measurements of the distribution of arsenic +III and +V species in binary mixtures and in a complex sample. De Smet et al. [14] proposed a methodology involving the differentiation of the mixed oxides and of mixture of praseodymium and molybdenum oxides by TOF s-SIMS. The distribution and the presence of specific ions, mainly in negative ions allowed these authors to follow the surface modifications of a Pr_6O_{11} – MoO_3 catalyst, used in the oxidation of isobutene. With a purpose of speciation, some groups carried out investigations related to the study of more complex systems (e.g. alkaline and alkaline earth salts). In addition to the works of our laboratory [20–23] and those of Denemont and Landry [31], it consists mainly of studies undertaken at the University of Answers [25,31–37]. First carried out with TOF-LMMS microprobe [32–34], they were later achieved by a FTICRMS laser microprobe [25,35,36], and more recently by the s-SIMS technique [36,37]. All these works show the potential of the laser microprobe mass spectrometers and s-SIMS instruments in the inorganic compound characterization. Moreover, a comparative study of results obtained by TOF-LMMS, FTICRMS, and s-SIMS in the examination of hexavalent molybdenum oxide and of sodium sulfate are proposed [30] and led these authors to regard these three techniques as complementary. Moreover, they also consider that

the strict application of the Plog model [1] does not allow efficient speciation of mineral compounds.

Recently, Oliveira et al. [38] published a FTICRMS study concerning the negative cluster ions produced by laser ablation/ionization of various transition metal oxides at the 1064 nm wavelength. At this wavelength, the comparative analysis of the negative cluster ions observed as fingerprints of MnO , Mn_2O_3 , Mn_3O_4 , and MnO_2 on the one hand, and of Fe_2O_3 and Fe_3O_4 on the other hand, does not make it possible to distinguish these various manganese and iron oxides; this contrasts the results obtained when a shorter wavelength is used [28–30,35]. Considering these results, it appears clearly that it is necessary to use wavelengths in the UV range to ensure a significant difference on the fingerprints for oxides at various stoichiometry. Consequently, after the evaluation of the Plog model to the differentiation of the chemical state of chromium compounds by UV-LA-FTICRMS technique, we will show its limitations especially when the reference compounds selected do not only correspond to oxides. In this case, we will show that knowledge of the formation mechanisms for the ionic species [39] ensures, due the choice of more adequate criteria of speciation, the establishment of a more reliable methodology. Indeed, we will show that the differentiation of the chromium compounds may be carried out by considering only two ion intensity ratios. Finally, we will determine how some oxides, free of chromium could lead to a modification of the methodology proposed. Finally, the study of matrix effect will allows us to determinate the limitations in the application of these new methodology of chromium speciation for the examination of polyphasic matrix.

2. Experimental

2.1. Chemicals

All commercial chemicals were of analytical reagent grade. Lithium chromate (94%) was purchased from Sigma (St. Louis, MO, USA), chromium (VI) oxide (99%), chromium (III) oxide (98%), chromium

(III) sulfate (99%), chromium (III) nitrate (99%), ammonium dichromate (99%), sodium chromate (99%), and chromium potassium sulfate dodecahydrate (98%) were purchased from Aldrich (Milwaukee, MI, USA); potassium chromate (99.5%) and lead chromate (99%) from Fluka (Buchs, Germany); rubidium, cesium, and calcium chromate with a purity of 99.9% from Cerac (Milwaukee, WI, USA); Nickel chromite (90%) from Alfa (Karlsruhe, Germany); potassium dichromate (98%) from Prolabo (Paris, France). Magnesium, strontium, and barium chromate were prepared according to the methods described elsewhere [39a], iron, zinc and manganese chromite according to the method described by Manoharan [40]. The $Zn_2(OH)_2CrO_4$ and silver chromate were prepared according to the classical method described by Pascal [41].

2.2. Laser microprobe Fourier transform ion cyclotron resonance mass spectrometer system

These analyses were performed using a laser microprobe FTICR mass spectrometer that has been described in detail elsewhere [42,43]. This instrument is a modified differentially pumped, dual-cell Nicolet Instrument FTMS 2000 (Finnigan FT/MS, now named ThermoQuest, Madison, WI, USA) operated with a 3.04 T magnetic field and coupled to a reflection laser interface. The viewing system, using an inverted Cassegrain optics design, allows the visualization of the sample with 300-fold magnification. A new sample probe fitted with motorized micromanipulators into the three spatial directions allows to achieve a spatial accuracy of less than 10 μm . The ionization step was performed using the third harmonic of a Q-switch Nd-YAG laser ($\lambda = 355 \text{ nm}$, pulse duration 4.3 ns, output energy used 0.8 mJ). The diameter of the laser beam on the sample (placed inside the source cell just in front of the source trap plate and kept at a ground potential) can be adjusted by means of the internal lens and an external adjustable telescope from five to several hundred micrometers, which corresponds to a power density ranging from 10^{10} to 10^6 W/cm^2 . The experiment sequence used for these analyses is as follows:

Table 1

FTICRMS parameters for an analytical sequence used to perform the differentiation of chromium compounds in negative detection mode at $\lambda = 355 \text{ nm}$

Power density	$5 \times 10^7 \text{ W/cm}^2$
Ionization sequence	Trapping potential: -3.5 V Ionization time: 1 ms Delay: 0 s
Ejection sequence	None
Excitation sequence	Trapping potential: -3.5 V Mass range: 70–750 Sweep rate: 1500 Hz/ μs Attenuation of excite rf: 0 dB
Detection sequence	Trapping potential: -3.5 V Acquisition frequency: 4000 Hz Attenuation of detected signal: 10 dB Number of data points: 32 kB

ions are formed by laser ablation in the source cell (residual pressure $\sim 10^{-5} \text{ Pa}$). During the ionization event, the conductance limit plate between the two cells and the source trap plate is fixed at a trapping potential of typically 2 V (respectively, -2 V in negative detection mode) or at a lower potential in some particular applications (down to 0.25 V). A variable delay period follows, during which ion/molecule reactions can occur. Ions are then excited by a frequency excitation chirp and the resulting image current is detected, amplified, digitized, apodized (Blackman-Harris, three-terms) and Fourier transformed to produce a mass spectrum.

More precisely, a FTICRMS sequence consists of a succession of events [44], which control the processes leading to the formation of the ionic species to the detection of generated ions. The modification of the FTICRMS sequence parameters greatly influences the nature and the distribution of the ions on the mass spectra.

However, parts of the slice of the analytical sequence are seldom modified. Practically, the optimization of a FTICRMS analytical sequence consists in the adjustment of almost fifteen parameters. Moreover, if selective ejections of very abundant ions are needed the modulation of three new parameters with each ejection sequence is necessary. An example of an analytical sequence used in this work is given in Table 1.

Note that a large part of the experiment was performed in the positive detection mode with Cr^+ and M^+ ejection [45] (where M is the counter ion of

the chromate or chromite compounds) in order to enhance the detection of the signal delivered by mixed oxygenated cluster ions. In fact, all atomic ions are likely to induce a dissociation of cluster ions by collision and therefore disturb the detection of the latter. Indeed, the (partial or total) ejection of the large majority of atomic ions allows an increase in the potentiality to detect large cluster ion and this without any loss of information in the conditions of our investigation. Each FTICR mass spectrum resulted from an average of one hundred laser shots fired on consecutive spots to obtain an acceptable reproducibility on the relative intensities of the ions. Furthermore, the sample is moved continuously during the experiment using the motorized micromanipulators of our device in x and y directions to analyze a fresh surface at each laser shot. Measuring the exact masses, after calibrating and identifying the isotopic distribution, assists in the ion assignments.

2.3. Preparation of the mixture pellets

The samples are made of a 200 mg pellet (precision: ± 0.1 mg). The two components of the mixture are then ground carefully for 15 min in an agate mortar before being conditioned into pellet under a pressure of $3t/cm^2$ for 15 min. The same procedure was used to prepare the pellets of the standard chromium compounds.

2.4. Model of Plog

An empirical formula for the absolute yields of secondary ions emitted from an oxidized metal surface or a metal oxide has been developed by Plog et al. [1]. The intensity of distribution for both positive and negative ions with different metal atom and oxygen content could be fitted by Gaussian functions which can be adequately described by two parameters, i.e. the location of the maximum and the width of the distribution. Specifically, the logarithm of the ion intensity is plotted versus the formal valence defined for $M_pO_n^q$ ions as $K = (q + 2n)/p$ when assigning the valence -2 to oxygen. These curves have been

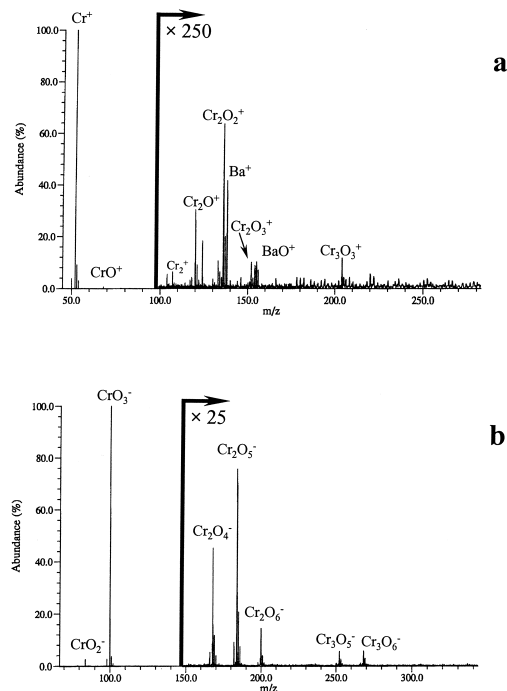


Fig. 1. (a) Positive and (b) negative LA-FTICR mass spectra of Cr_2O_3 at a wavelength of 355 nm, with a power density of 5×10^7 W/cm^2 .

referred to as Plog curves; they look like parabola when plotted as a function of the fragment valence K :

$$I_{rel}^{\pm}(K) = I_{max}^{\pm} \exp\left(-\frac{(K - G^{\pm})^2}{\gamma^2}\right) \quad (1)$$

with I_{max}^{\pm} : maximum intensity of the fitted curve; G^{\pm} : K value corresponding to the maximum intensity; γ^2 : variance of the distribution (γ is the width of the intensity distribution taken at $e^{-0.5}$ of the Plog curve maximum expressed in K values).

3. Results and discussion

3.1. Evaluation of the application of the Plog model in the speciation of chromium compounds

To evaluate the capability of the Plog model for the differentiation of various chromium compounds, experiments using trivalent and hexavalent oxides and

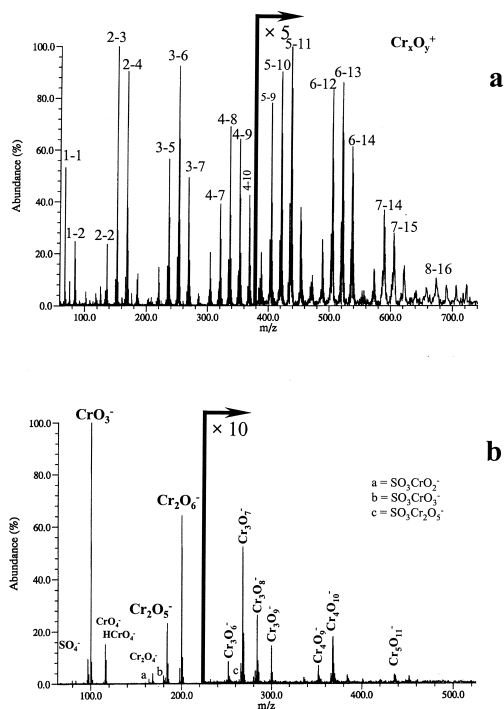


Fig. 2. (a) Positive and (b) negative LA-FTICR mass spectra of $\text{Cr}_2(\text{SO}_4)_3 \cdot x\text{H}_2\text{O}$ at $\lambda = 355$ nm, with a power density of 3×10^7 W/cm^2 .

for hydrated trivalent sulfate were conducted. For all of these three chromium compounds, the cluster ions detected in both positive and negative ion mode come from the $\text{Cr}_x\text{O}_y^{+/-}$ families (Figs. 1, 2, and 3, respectively). Depending on the nature of the compound studied, the number and the type of cluster ions (i.e. the Cr/O ratio in the ion) are different. In particular, ions detected in the study of the trivalent chromium oxide are less oxygenated than those observed for hexavalent chromium oxide and hydrated trivalent chromium sulfate. For the latter, the cluster ions detected especially in positive detection mode are more abundant. Hydrogenated species are also detected.

For the three chromium compounds, Plog curves are obtained (see Fig. 4) and allowed the calculation of the Plog parameters G^+ , G^- , and G_0 (Table 2) for various ion series. The lattice valence G_0 is globally independent of the nature of the $\text{Cr}_x\text{O}_y^{+/-}$ series but closely dependent of the nature of the studied compound. The G_0 parameter is equal to

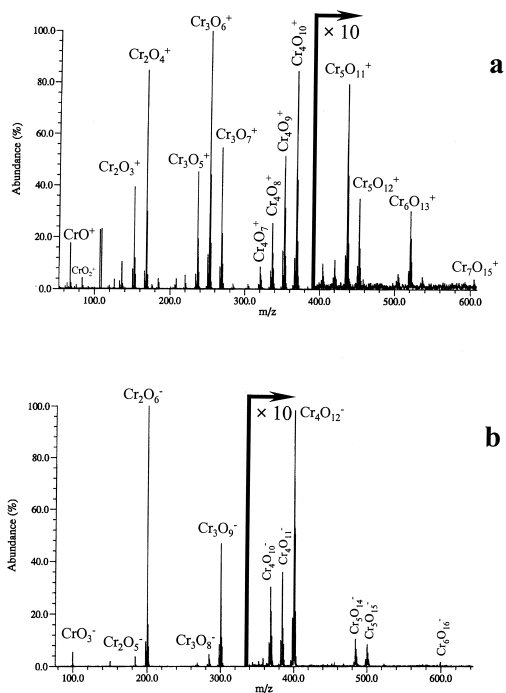


Fig. 3. (a) Positive and (b) negative LA-FTICR mass spectra of CrO_3 at $\lambda = 355$ nm, with a power density of 3.6×10^{10} W/cm^2 .

3.2, 4.3, and 5.0 for Cr_2O_3 ; $\text{Cr}_2(\text{SO}_4)_3 \cdot x\text{H}_2\text{O}$; and CrO_3 , respectively. As expected, in the case of Cr_2O_3 , G_0 depends more on the nature and on the relative proportion of the CrO_2 and CrO_3 neutrals involved in the formation of the $\text{Cr}_x\text{O}_y^{+/-}$ (see Secs. 3.2.4 and 3.3.1) than on the chromium chemical state in the studied compound.

When considering these results, the transposition of the Plog model to the laser ablation/ionization mass spectrometry seems to be a reliable method for the distinction of the three chromium compounds, even if it does not allow to assign their true oxidation state. The generalization of the transposition of the Plog model to the study of the other standard compounds was attempted. Unfortunately a great part of them, especially chromate ones, leads to the formation, in positive ions of $\text{M}_n\text{Cr}_x\text{O}_y^+$ mixed metal cluster ions instead of Cr_xO_y^+ ones. Consequently the transposition of the Plog model can not be generalize for all of the 19 chromium reference compounds selected due to the fact that G^+ cannot be calculated. This is the reason why an alternative methodology was investigated.

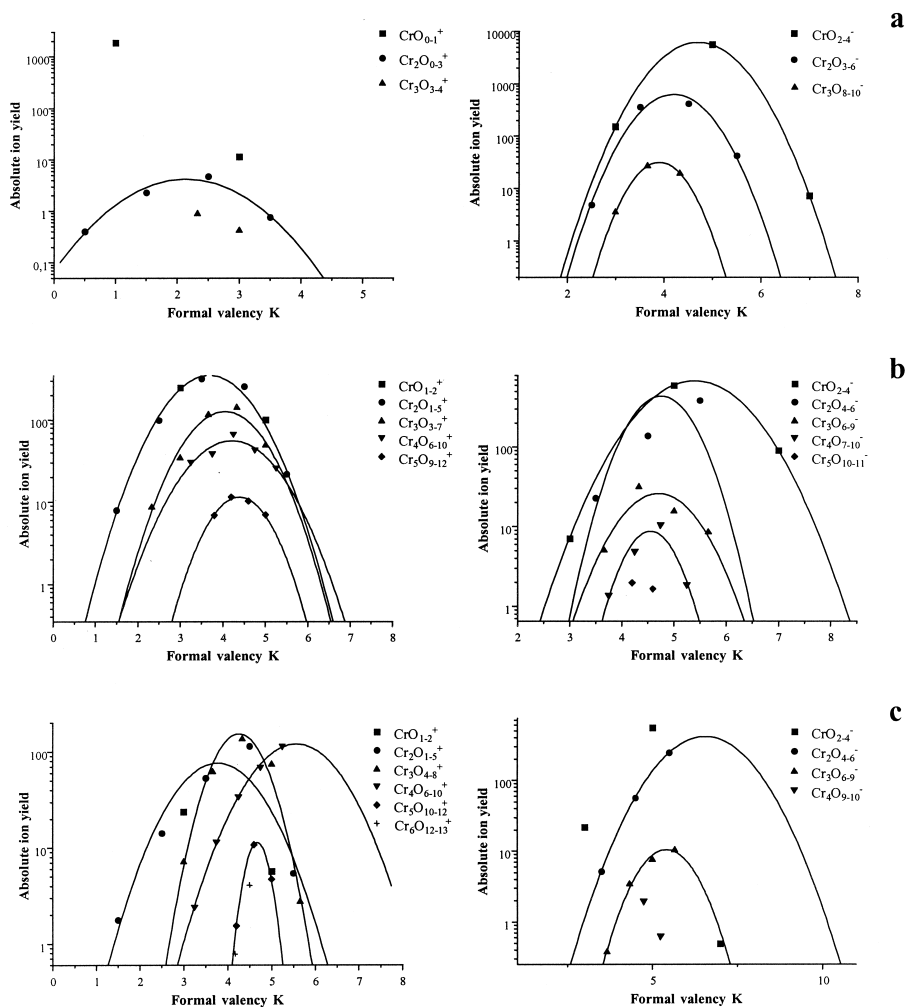


Fig. 4. Plog curves obtained from LA-FTICR mass spectra from (a) Cr_2O_3 , (b) $\text{Cr}_2(\text{SO}_4)_3 \cdot x\text{H}_2\text{O}$, and (c) CrO_3 at $\lambda = 355 \text{ nm}$, with a power density 5×10^7 , 5×10^7 , and $3.6 \times 10^{10} \text{ W/cm}^2$, respectively.

3.2. Establishment of a new methodology for the differentiation of chromium chemical state

3.2.1. Fingerprint of chromium compounds

The study of the various reference compounds in the positive ion detection mode led to the observation of many oxygenated mixed cluster ions $\text{M}_x\text{Cr}_y\text{O}_z^+$, in particular in the analysis of the alkali and alkaline earth chromates [39a] and of chromite compounds. The diversity of these positive cluster ions does not allow an easy comparison of the results obtained and

makes it difficult to propose a methodology based on the distribution of the positive cluster ions.

On the opposite, many similarities appear when the experiments are carried out in the negative ion mode. Indeed, Cr_xO_y^- cluster ions are observed in the negative mass spectra for all reference chromium compounds. That is the reason why this mode of detection was retained to establish a protocol for the differentiation of +III and +VI chemical state of chromium. The Cr_xO_y^- ions are limited to the $\text{Cr}_3\text{O}_{5-9}^-$ ones for chromates and chromites. However, the production of

Table 2

G^+ , G^- , and G_0 Plog parameters for Cr_2O_3 , $\text{Cr}_2(\text{SO}_4)_3 \cdot x\text{H}_2\text{O}$, and CrO_3 chromium compounds obtained in the study of various $\text{Cr}_x\text{O}_y^{+/-}$ series at $\lambda = 355$ nm with a power density of 5×10^7 , 3×10^7 , and 3.6×10^{10} W/cm², respectively

Ions	Cr_2O_3			$\text{Cr}_2(\text{SO}_4)_3 \cdot x\text{H}_2\text{O}$			CrO_3		
	G^+	G^-	G_0	G^+	G^-	G_0	G^+	G^-	G_0
$\text{CrO}_y^{+/-}$		4.70			5.40				
$\text{Cr}_2\text{O}_y^{+/-}$	2.14	4.20	3.17	3.68	4.76	4.22	3.78	6.56	5.17
$\text{Cr}_3\text{O}_y^{+/-}$		3.90		4.05	4.71	4.38	4.27	5.42	4.84
$\text{Cr}_4\text{O}_y^{+/-}$				4.22	4.56	4.39	5.57		
$\text{Cr}_5\text{O}_y^{+/-}$				4.39			4.68		

species containing up to 5 or 6 chromium atoms is observed in the analysis of hexavalent chromium oxide CrO_3 and hydrated trivalent chromium salts (nitrate and sulfate). The laser ablation/ionization of the latter also leads to a significant formation of hydrogenated cluster ions (HCrO_4^- , HCr_2O_7^- , $\text{HCr}_3\text{O}_{10}^-$, $\text{HCr}_4\text{O}_{13}^-$, and $\text{HCr}_5\text{O}_{16}^-$ ions as in Fig. 2). This characteristic seems to be related to a significant presence of water molecules in these compounds. The significant production of HCrO_4^- when the zinc hydroxychromate is studied confirms the strong dependence between the production of these hydrogenated species and the presence of hydrogen atoms in the structure of the analyzed compound. Indeed, the examination of mixtures between sodium decahydrated sulfate and trivalent chromium oxide clearly indicates an increase in the intensity for the HCrO_4^- ion [21]. Moreover, the mass spectrometry study of various hydration degrees for $\text{KCr}(\text{SO}_4)_2 \cdot x\text{H}_2\text{O}$ chromium alum clearly shows a strong dependence of this hydration degree on the relative intensity of CrO_4^- and HCrO_4^- ions [46]. These two studies confirmed our conclusion.

3.2.2. Influence of instrumental parameters

To evaluate the importance of the laser wavelength on the relative distribution for the negative ions, a

study with hexavalent oxide CrO_3 at three wavelengths: 193 (ArF excimer laser, pulse duration 23 ns), 266 (quadrupled Nd-YAG laser, pulse duration 4.3 ns), and 355 nm (tripled Nd-YAG laser, pulse duration 4.3 ns) was done. The results are displayed in Table 3. For a laser power density of $I = 3 \times 10^7$ W/cm², the hexavalent chromium oxide leads for these three different wavelengths to a same fingerprint. Indeed, the processes involved in the formation of the negative ions are less wavelength dependent than the processes observed with positive ions [39b]. However, as the photon energy increase (i.e. decrease of the wavelength) leads overall to a decrease of the absolute intensity of the signal. This explains why the following experiments were carried out at the wavelength of 355 nm, to improve the sensitivity of the detection. Further, depending of the electronic density of the gaseous cloud, the ion distribution in the negative ion detection mode depends strongly on the power density [47]. Indeed CrO_2^- and CrO_3^- precursor ions in particular may be produced by electronic capture according to their high electron affinity (2.41 and 3.41 eV, respectively [48]). Moreover, a great power density is in favor of some multiphoton absorption processes, which induce an accumulation of

Table 3

Cr_xO_y^- cluster ions detected in the study of hexavalent chromium oxide vs. the wavelength used at a power density of 3×10^7 W/cm² (abundance given in percent); in parentheses for the Cr_2O_6^- ion, its absolute abundance in arbitrary unity

Wavelength (nm)	CrO_3^-	Cr_2O_5^-	Cr_2O_6^-	Cr_3O_7^-	Cr_3O_8^-	Cr_3O_9^-	$\text{Cr}_4\text{O}_{10}^-$	$\text{Cr}_4\text{O}_{11}^-$	$\text{Cr}_4\text{O}_{12}^-$
193	7	4	100 (171.2)	1	5	45	3	4	10
266	26	10	100 (280.4)	1	3	17	1	1	3
355	12	3	100 (341.9)	2	6	26	5	4	6

Table 4
 Cr_xO_y^- cluster ions detected in the study of zinc chromite at $\lambda = 355$ nm vs. the power density used 3×10^7 W/cm², relative intensity in percent

Power density (W/cm ²)	CrO_2^-	CrO_3^-	Cr_2O_4^-	Cr_2O_5^-	Cr_2O_6^-
3×10^8	10	100	9	5	1
5×10^7	5	100	5	10	6
1.6×10^7	...	100	5	26	27

internal energy of the ions and consequently an increase of the dissociation processes. These two factors are responsible for the changes in the distribution of ions, more particularly for the mass spectrum of zinc chromite ZnCr_2O_4 . Under 355 nm, with a power density between 3×10^8 and 1.6×10^7 W/cm² (Table 4), a significant increase of ions with a great m/z ratio is in particular observed at low power density with a decrease of the CrO_2^- ion. That is the reason why the comparison between the mass spectra of the various reference compounds must be carried out at a similar value of power density. Taking into account the results obtained in the preliminary studies we chose to carry out the following experiments at a power density of 5×10^7 W/cm². Further, preliminary analyses of the 19 standard chromium compounds have resulted in the determination of the optimal experimental condition (power density and FTICRMS analytical sequence) for each of them. These optimum conditions vary sometimes quite strongly from one reference compound to another one. Further, as previously explained in sec. 2, the nature of the instrumental parameters greatly influences the ion distribution on the mass spectra. This explains why a new set of experiments performed with exactly the same experimental conditions (i.e. same FTICRMS analytical sequence and under same laser power density) is required for all of the chromium reference compounds. However, if a common analytical sequence is used as a compromise, it does not need to be an optimal one for the analysis of all of the compounds. After considering various experimental sequences, the parameters displayed in Table 1 have been chosen. Note that all of the following results in this article have been obtained in the negative ion mode by

using these experimental conditions. Moreover, the pressure in the source cell is for all experiments kept between 10^{-5} and 1.8×10^{-5} Pa.

3.2.3. Strategy for the study of the fingerprints of chromium reference compounds

The importance of a given Cr_xO_y^- cluster ion series in the negative ion mode detection is strongly related to the power density used (see Sec. 3.2.2). A comparison of the intensity of CrO_y^- ions of the first generation to Cr_2O_y^- ions of the second one for example would be discutable. Moreover, considerations of the level of lattice energy of the compound studied may also be taken into account to explain the evolution of mass spectra. Weaker lattice energies are more favorable for the formation of greater cluster ions. The comparison of the intensity of a given ion compared to another one within the same ion generation (ions with the same number of chromium atoms) is more powerful to provide structural information. Indeed, the relative distribution of the cluster ions is directly connected to the Cr/O ratio in the studied compound. The intensity of each ion is normalized to the sum of the intensity of the ions which included the same number of chromium atoms. Statistical data on the repeatability of the results are obtained by considering 20 consecutive experiments (Table 5).

3.2.4. Method for differentiate chromium compounds

The examination of the anhydrous compounds of trivalent chromium and hexavalent chromium makes it possible to highlight the strong dependence of the formation of the cluster ions with respect to the valence of chromium in the reference compounds. The hexavalent chromium oxide and the chromate compounds lead to a significant formation of ionized clusters strongly oxygenated. On the contrary, the trivalent compounds are in favor of the formation of more slightly oxygenated species. This observation was checked more particularly when the $\text{Cr}_2\text{O}_{4-6}^-$ cluster ions are considered. The production of the Cr_2O_4^- ions is more significant in the case of the chromite and trivalent chromium oxide experiments whereas the production of Cr_2O_6^- favors for hexava-

Table 5

Distribution of the $(\text{H})_{0-1}\text{Cr}_{1-2}\text{O}_y^-$ cluster ions observed on the mass spectra of the chromium reference compounds at a wavelength of 355 nm with a power density of $5 \times 10^7 \text{ W/cm}^2$ by using the standard FTICRMS analytical sequence.

Compounds	Cluster ions								
	CrO_2^-	CrO_3^-	CrO_4^-	HCrO_4^-	Cr_2O_4^-	Cr_2O_5^-	Cr_2O_6^-	Cr_2O_7^-	HCr_2O_7^-
Li_2CrO_4	0.3 ± 0.1	99.0 ± 0.1	0.4 ± 0.08	0.3 ± 0.09	2.2 ± 0.7	35.2 ± 7.9	61.5 ± 8.5	1.0 ± 0.2	
Na_2CrO_4	0.04 ± 0.01	98.0 ± 0.1	0.9 ± 0.1	0.6 ± 0.07	0.8 ± 0.1	27.0 ± 1.9	72.1 ± 1.9		
K_2CrO_4	0.02 ± 0.01	99.3 ± 0.2	0.5 ± 0.2	0.1 ± 0.02		22.5 ± 2.6	77.5 ± 3.0		
Rb_2CrO_4	0.1 ± 0.1	99.2 ± 0.2	0.3 ± 0.07	0.4 ± 0.2		19.0 ± 2.4	81.0 ± 2.5		
Cs_2CrO_4	0.1 ± 0.8	99.4 ± 0.3	0.3 ± 0.15	0.1 ± 0.1		21.6 ± 9.9	78.4 ± 9.9		
$\text{MgCrO}_4 \cdot 5\text{H}_2\text{O}$	1.10 ± 0.08	96.6 ± 0.9		2.3 ± 0.5		2.4 ± 0.4	97.6 ± 0.4		
CaCrO_4	2.9 ± 0.4	95.7 ± 0.4	0.8 ± 0.1	0.2 ± 0.05	5.8 ± 0.9	41.5 ± 2.2	52.7 ± 2.8		
SrCrO_4	1.5 ± 0.2	98.1 ± 0.2	0.3 ± 0.1	0.2 ± 0.05	12.3 ± 4.7	54.7 ± 4.6	33.0 ± 6.0		
BaCrO_4	1.0 ± 0.2	98.4 ± 0.2		0.5 ± 0.1	4.3 ± 0.8	33.9 ± 4.7	61.8 ± 5.3		
PbCrO_4	0.6 ± 0.3	98.2 ± 0.2		1.2 ± 0.6	0.2 ± 0.1	13.7 ± 2.7	86.1 ± 2.7		
$\text{Zn}_2(\text{OH})_2\text{CrO}_4$		91.4 ± 6.4		8.6 ± 6.4		6.7 ± 3.8	91.8 ± 3.7		
Cr_2O_3	2.9 ± 0.6	96.9 ± 0.5	0.2 ± 0.1		35.3 ± 2.5	58.7 ± 1.9	5.9 ± 0.1		
CrO_3	2.8 ± 1.6	96.9 ± 1.5	0.1 ± 0.1	0.1 ± 0.1	3.7 ± 1.4	24.8 ± 7.8	71.5 ± 8.5		
$\text{Cr}_2(\text{SO}_4)_3$	0.6 ± 0.2	84.7 ± 3.3	7.9 ± 1.9	6.8 ± 1.5	10.2 ± 3.9	34.8 ± 4.0	54.0 ± 7.0	0.5 ± 0.2	0.6 ± 0.2
$\text{Cr}(\text{NO}_3)_3$		36.9 ± 3.7		63.1 ± 3.7		0.1 ± 0.4	75.1 ± 3.7		24.8 ± 3.8
FeCr_2O_4	2.8 ± 1.1	97.1 ± 1.2		0.1 ± 0.1	31.5 ± 5.8	56.2 ± 6.5	12.3 ± 4.1		
MnCr_2O_4	12.1 ± 2.4	87.8 ± 2.4			51.1 ± 3.3	46.4 ± 3.8	3.5 ± 1.5		
NiCr_2O_4	4.6 ± 3.3	95.3 ± 3.3		0.1 ± 0.1	34.9 ± 4.5	52.4 ± 6.1	12.7 ± 5.4		
ZnCr_2O_4	3.6 ± 1.3	96.0 ± 1.2	0.1 ± 0.1	0.3 ± 0.1	23.5 ± 3.0	50.3 ± 4.5	26.1 ± 5.0		

lent compounds (Table 5). These observations are in agreement with the results obtained in the differentiation of MoO_2 – MoO_3 [27], FeO – Fe_2O_3 – Fe_3O_4 [28–30], and PbO – PbO_2 [9], respectively, for which the production of strongly oxygenated cluster ions is characteristic of a valence increase for the metal in the studied oxide. These observations must be related to the mechanism of formation of the $\text{Cr}_2\text{O}_{4-6}^-$ cluster ions. These ions result from aggregation processes between CrO_2 or CrO_3 neutrals and CrO_2^- or CrO_3^- precursor ions. The Cr_2O_4^- ion may equally be considered as a combination of CrO_3 neutral and CrO^- ion, even if this latter is not detected on the LA-FTICR mass spectra of the chromium compounds analyzed. Indeed, it may be assumed, that the kinetics of aggregation is too fast to allow its observation. Further, a smaller electron affinity of the CrO neutral (1.22 eV [48]) comparing to CrO_2 and CrO_3 neutral species may also explained the lack of the CrO^- ion. Considering the aggregative pathways involving the

other precursor ions CrO_2^- and CrO_3^- , it is reasonable to think that aggregation processes between CrO^- and CrO_2 may lead to the formation of the Cr_2O_3^- according to what it was observed in previously TOF-LMMS study of trivalent chromium oxide [21]. However this latter ion is not detected in LA-FTICRMS experiments (Fig. 1), this is why the occurrence of aggregation processes involving CrO^- and CrO_2 or CrO_3 neutrals may be neglected, in particular the contribution of the CrO_3CrO^- component in the production of the Cr_2O_4^- ion.

Finally, a greater production of CrO_2^- ions and CrO_2 neutrals is favorable as compared to the formation of Cr_2O_4^- ion in the case of anhydrous trivalent compound study. On the other hand, the formation of higher oxygenated ionic and neutral species, respectively, CrO_3^- and CrO_3 ones for hexavalent chromium compounds lead to the preferential formation of the Cr_2O_6^- ions. A methodology based on the calculation of the intensity ratio $R_1 = I(\text{Cr}_2\text{O}_4^-)/I(\text{Cr}_2\text{O}_6^-)$ ions

Table 6
 R_1 and R_2 intensity ratios calculated for the various chromium reference compounds.

Compound	Ratio	
	R_1	R_2
CrO ₃	0.055 ± 0.011	0.003 ± 0.002
Li ₂ CrO ₄	0.038 ± 0.003	0.007 ± 0.002
Na ₂ CrO ₄	0.011 ± 0.001	0.015 ± 0.001
K ₂ CrO ₄	0	0.007 ± 0.002
Rb ₂ CrO ₄	0	0.007 ± 0.002
Cs ₂ CrO ₄	0	0.004 ± 0.002
MgCrO ₄	0	0.024 ± 0.005
CaCrO ₄	0.11 ± 0.02	0.014 ± 0.003
SrCrO ₄	0.41 ± 0.08	0.005 ± 0.002
BaCrO ₄	0.07 ± 0.02	0.005 ± 0.001
PbCrO ₄	0.002 ± 0.001	0.012 ± 0.006
Zn ₂ (OH) ₂ CrO ₄	0	0.10 ± 0.02
Cr ₂ O ₃	6.0 ± 1.30	0.0016 ± 0.0003
FeCr ₂ O ₄	2.8 ± 0.8	0.002 ± 0.001
MnCr ₂ O ₄	16.0 ± 3.8	0 ± 0
NiCr ₂ O ₄	3.3 ± 0.9	0.0006 ± 0.001
ZnCr ₂ O ₄	1.0 ± 0.2	0.004 ± 0.002
Cr ₂ (SO ₄) ₃ , xH ₂ O	0.20 ± 0.04	0.18 ± 0.03
Cr(NO ₃) ₃ , 9H ₂ O	0	1.7 ± 0.2

may allow to distinguish the trivalent and the hexavalent chromium compounds. Nevertheless, examination of hydrated chromium salts disturbs this methodology. Indeed, for sulfate or nitrate compounds, the value of the ratio $R_1 = I(\text{Cr}_2\text{O}_4^-)/I(\text{Cr}_2\text{O}_6^-)$ is equal to 0.20 and 0 respectively. It will identify, in a first step, these compounds as hexavalent chromium compounds. To avoid a wrong identification, however, it is necessary to employ a second criterion of speciation. As previously noted, the great production of hydrogenated species is one of the characteristics of the hydrated trivalent chromium compounds. This is why the second criterion takes into account this kind of ions. Indeed, the calculation of the intensity ratio $R_2 = [I(\text{CrO}_4^-) + I(\text{HCrO}_4^-)]/I(\text{CrO}_3^-)$ makes it possible to clearly distinguish the hydrated trivalent chromium compounds from the hexavalent ones. Both R_1 and R_2 intensity ratios for all chromium reference compounds are shown in Table 6.

These results enable us to propose a methodology for the differentiation of the chromium chemical state (Fig. 5). When our new methodology is compared to

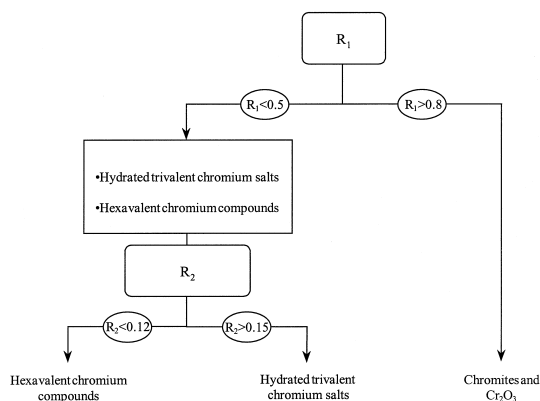


Fig. 5. Speciation for trivalent, hydrated trivalent, and hexavalent chromium compounds by LA-FTICRMS at $\lambda = 355$ nm, with a power density of 5×10^7 W/cm².

those procedures established previously with TOF-LMMS experiments by Poitevin et al. [20], some differences become obvious. Due to a high abundance of the CrO_2^- ion, Poitevin et al. included these ions in their methodology, which mainly considered the ions of the first generation. Moreover, the analytical protocol established here is simpler and more reliable because it is established after the analysis of a greater range of reference compounds. Further, a better control of the power density used in a FTICRMS experiment adds to the reliability of the methodology.

To evaluate this new methodology of differentiation of the chromium chemical state, it was applied to the study of several compounds: FeCr_2O_4 (prepared according to a methodology alternative to the Manoharan one); $\text{KCr}(\text{SO}_4)_2 \cdot x\text{H}_2\text{O}$, Ag_2CrO_4 , $\text{K}_2\text{Cr}_2\text{O}_7$, $(\text{NH}_4)_2\text{Cr}_2\text{O}_7$, and a green commercial pigment. The results of the analysis of these compounds are reported in Table 7. Concerning the pure chromium compounds, the methodology proposed in this study allows an adequate assignment of the chromium chemical state. Indeed, the calculation of both R_1 and R_2 ratio leads to a positive diagnostic of chromium speciation. Further, when the green pigment is studied, the distribution of negative chromium anions [Fig. 6(a)] allows to assign an anhydrous trivalent chromium character to this compound. This diagnostic is confirmed on the one hand by the distribution of the $\text{Cr}_2\text{O}_{1-3}^+$ ions in positive detection mode [Fig.

Table 7

R_1 and R_2 intensity ratios obtained in the study of the FeCr_2O_4 , $\text{KCr}(\text{SO}_4)_2 \cdot x\text{H}_2\text{O}$, Ag_2CrO_4 , $\text{K}_2\text{Cr}_2\text{O}_7$, and $(\text{NH}_4)_2\text{Cr}_2\text{O}_7$ compounds and in the study of a commercial pigment.

Compounds	R_1	R_2	Assignment
FeCr_2O_4	2.93 ± 0.38	0.0050 ± 0.0004	Cr(III)
$\text{KCr}(\text{SO}_4)_2 \cdot x\text{H}_2\text{O}$	0.013 ± 0.004	0.14 ± 0.01	Hydrated Cr (III)
Ag_2CrO_4	0.010 ± 0.003	0	Cr(VI)
$\text{K}_2\text{Cr}_2\text{O}_7$	0.0018 ± 0.0006	0.007 ± 0.003	Cr(VI)
$(\text{NH}_4)_2\text{Cr}_2\text{O}_7$	0.014 ± 0.003	0.012 ± 0.001	Cr(VI)
Green pigment	12.2 ± 1.6	0	Cr(III)

6(b)] which is the same that observed for trivalent chromium oxide and on the other hand by the green color of this pigment.

3.3. Study of matrix effects

The great diversity of the processes taking place during the laser ablation/ionization leads us to consider the possibility of a modification of the relationship between R_1 and R_2 ratios and the nature of the studied chromium compound. We studied the evolution of the fingerprint for the reference chromium compounds when they are in presence of various oxides in binary mixtures. More particularly, the development of the R_1 and R_2 intensity ratios versus first the nature of the added oxide and second the weight ratio between chromium compound and oxide free of chromium (CaO , SiO_2 , Fe_2O_3 , and ZnO). The

chromium compounds selected in this part of the study were potassium, calcium, and magnesium chromate; zinc hydroxy–chromate, trivalent chromium oxide, iron and zinc chromite, and hydrated trivalent chromium sulfate. It is not necessary to study all of the reference compounds as they have a similar behavior.

The nature of the 31 mixtures studied is reported in the Table 8. Some of these mixtures have been prepared and analyzed twice to evaluate the reproducibility of the pellet pressing procedure. In all cases, the difference in the intensity ratio R_1 and R_2 between the two experiments did not exceeded $\pm 15\%$, which approximately correspond to the dispersion of the measurements when a given pellet is under investigation.

The R_1 ratio is significantly influenced by the introduction of each one of these four free chromium oxides. Calcium and silicon oxides lead globally to an increase in this ratio whereas the Fe_2O_3 and the ZnO have an opposite effect. These considerations will be discussed in more detail in the following section. The R_2 ratio is weakly influenced by the presence of calcium, zinc, iron or

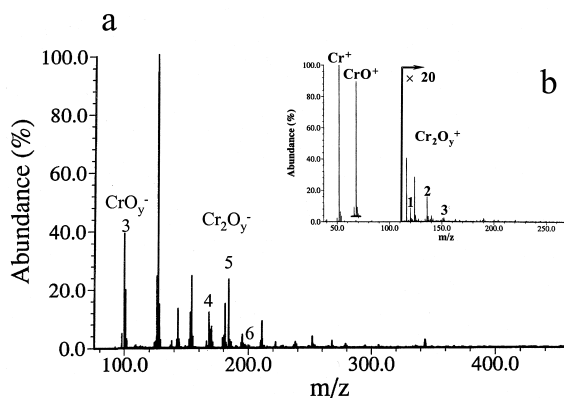


Fig. 6. (a) Negative and (b) positive LA-FTICR mass spectra of commercial green pigment at $\lambda = 355$ nm, with a power density of 5×10^7 W/cm^2 by using the standard instrumental sequence.

Table 8

Weight fraction of chromium compounds in the studied binary mixtures: chromium compounds–oxide containing no chromium

	ZnO	SiO_2	CaO	Fe_2O_3
K_2CrO_4	25	25	25	25
CaCrO_4	25	5–10–15–25–50		25
Cr_2O_3	25	25	25	25
FeCr_2O_4	25	5–10–15–25–50	10–25–50	
ZnCr_2O_4		25	25	25
$\text{Cr}_2(\text{SO}_4)_3 \cdot n\text{H}_2\text{O}$	25	25		
MgCrO_4		25		
$\text{Zn}_2(\text{OH})_2\text{CrO}_4$		25		

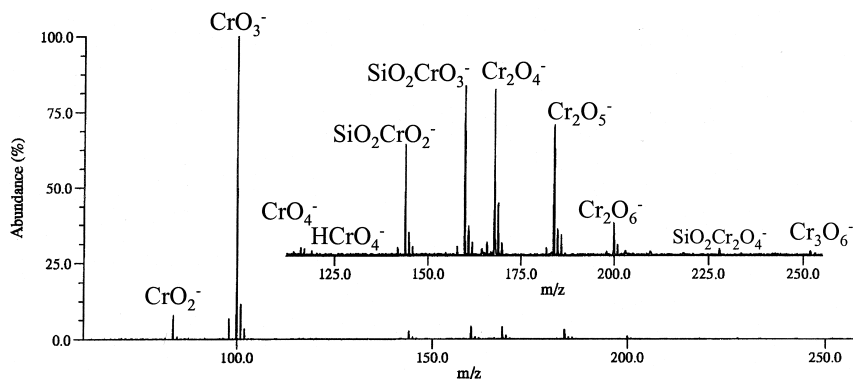


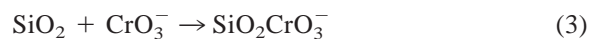
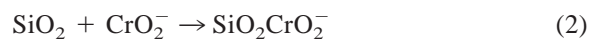
Fig. 7. Negative LA-FTICR mass spectra of a $\text{SiO}_2\text{-ZnCr}_2\text{O}_4$ mixture at $\lambda = 355$ nm, with a power density of 5×10^7 W/cm².

silicon oxides. However, in the case of the silica-hydrated trivalent chromium sulfate mixture a significant reduction of the production of the CrO_4^- ions and especially of the HCrO_4^- ones is observed. In fact, the production of this latter ion is disturbed by the production of a high number of hydrogenated cluster ions of silica [49].

3.3.1. Analysis of mixtures containing 25% in weight of chromium compounds

Whatever the chromium compound studied, the introduction of silicon and calcium oxides involves an increase of the R_1 ratio, which is connected to a reduction in the production of strongly oxygenated species in the gas cloud. This may be put in connection with the formation of mixed ions involving chromium, oxygen and silicon (respectively, calcium) atoms. Indeed, the analysis of the mixtures silica-chromium compounds (Fig. 7), lead in particular to the formation of $\text{SiO}_2\text{CrO}_2^-$ and $\text{SiO}_2\text{CrO}_3^-$ ions (respectively, at m/z 144 and 160) coming from aggregation of neutral SiO_2 on CrO_2^- and CrO_3^- precursor ions [reactions (4) and (5)]. Note the absence of SiO_2CrO^- ion at m/z 128 which strengthens the negligible importance of aggregative processes involving the CrO^- ion. However, these ions may equally result as aggregate processes occurring between oxygenated chromium neutrals and oxygenated silicon ions. The oxygenated chromium species (ion

or neutral) are also involved in the formation mechanisms of Cr_2O_4^- and Cr_2O_6^- ions [respectively, reactions (4) and (5)].



The introduction of competitive reactions of aggregation (2)–(5) involves changes in the mass spectra. Indeed, a different affinity from the CrO_2^- and CrO_3^- ions for the SiO_2 neutral or from the CrO_2 and CrO_3 neutrals for the SiO_2^- and SiO_3^- ions, induced a discrimination in the formation of the ions Cr_2O_4^- and Cr_2O_6^- ions and thus a disturbance of the R_1 ratio.

With regard to the analysis of the calcium oxide-chromium compound mixtures, the observation in the positive ion mode of mixed structures chromium-calcium-oxygen allows to make an analogy with the behavior of chromium compounds in the presence of silica. The cluster ions observed in this case (Fig. 8) are close to those met in the study of the calcium chromate [39a]. The formation of these latter leads to an oxygen deficiency of the gas cloud after the laser ablation and thus to a reduction in the production of cluster ions strongly oxygenated in negative mode of detection [39]. However, the R_1 ratio for binary

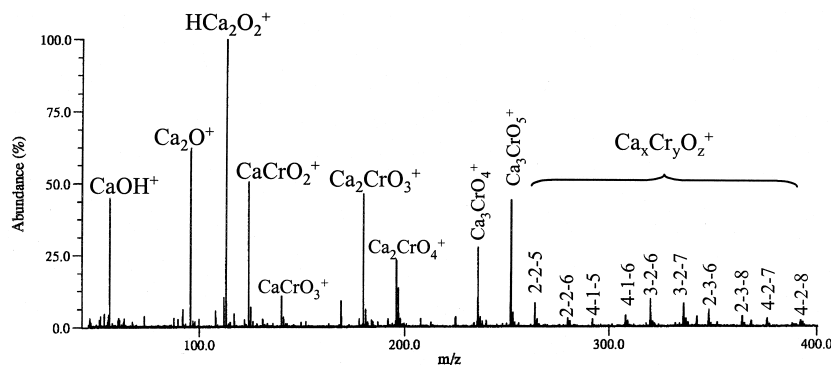


Fig. 8. Positive LA-FTICR mass spectra of a CaO–ZnCr₂O₄ mixture at $\lambda = 355$ nm, with a power density of 2.5×10^8 W/cm².

mixtures including 25% of hexavalent chromium compounds in weight is systematically down to 0.5 and allows to attribute the appropriate chemical state to chromium.

Contrary to the tendency observed for calcium and silicon oxides, trivalent iron oxide and zinc oxide support the production of strongly oxygenated ions. This leads to a significant reduction of the ratio R_1 and leads us to attribute a hexavalent character to anhydrous trivalent compounds (Table 9). However, if these two compounds lead to the same effect, two separate explanations must be exposed to account for their mechanisms of action.

The zincite ZnO leads to significant disturbances of the mass spectra. Indeed, for all of the studied mixtures a significant decrease of the production of the Cr_2O_4^- is observed to the benefit of Cr_2O_6^- . All in all, the presence of ZnO in the mixture results in the attribution of hydrated trivalent [for the $\text{Cr}_2(\text{SO}_4)_3 \cdot x\text{H}_2\text{O}$ –ZnO mixture] or hexavalent character for the studied mixtures whatever their nature. The explanation of such behavior must be related with the

mechanisms of ion formation. The study of zinc chromite leads to a similar observation. This compound presents indeed, the characteristic to provide contrary to other chromites, cluster ions of high generation in both modes of detection. The presence of zinc species in the gas cloud may support the processes of ion molecule reaction [50].

If the effect of the iron trivalent oxide is identical to that of ZnO, the processes involved are very different. Trivalent iron oxide constitutes in fact an oxygen stock for the formation of these highly oxygenated species. With regard to the enthalpy of formation of the oxygenated iron and chromium neutral species (Table 10), FeO, CrO, CrO₂, and CrO₃, respectively [51] it appears clearly, that during the laser ablation/ionization process, these latter are favored. Indeed, the laser ablation of a mixture of iron and chromium oxygenated compounds involves the formation of neutral species displayed in Table 10. A collision in the gas cloud between a chromium neutral (CrO_{0-2}) and a FeO neutral will lead thermodynamically to the iron–oxygen breaking bond following by

Table 9

R_1 intensity ratio observed for mixtures including zinc and trivalent iron oxides with anhydrous trivalent chromium compounds

	R_1 ratio
Cr ₂ O ₃ –Fe ₂ O ₃	0.17 ± 0.03
Cr ₂ O ₃ –ZnO	0.08 ± 0.04
ZnCr ₂ O ₄ –Fe ₂ O ₃	0.10 ± 0.03
FeCr ₂ O ₄ –ZnO	0.17 ± 0.06

Table 10

Enthalpy of formation for some iron and chromium oxygenated neutral species according to [51]

	Enthalpy of formation at 298.15 K (kJ/mol)
CrO _(g)	188.28
CrO _{2(g)}	–75.57
CrO _{3(g)}	–292.88
FeO _(g)	251.04

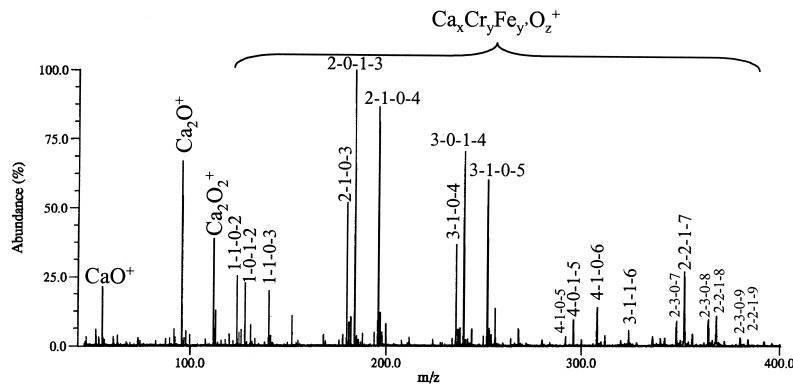
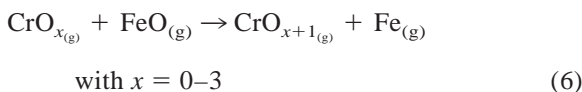


Fig. 9. Positive LA-FTICR mass spectra of a Fe_2O_3 – CaCrO_4 mixture at $\lambda = 355$ nm, with a power density of 2.5×10^8 W/cm^2 .

the capture of oxygen by the chromium neutral according to



The enthalpy of formation for $\text{Fe}_{(\text{g})}$ is equal to 415.47 kJ/mol at the temperature of 298.15 K [51]. Moreover, this conclusion is confirmed on the fingerprint of the iron chromite by the absence of aggregation relative to the FeO neutrals.

However, for the Fe_2O_3 – CaCrO_4 mixture an increase of the R_1 ratio was observed as opposed to what expected. The examination of the positive ion mass spectrum gives the explanation: iron–calcium–oxygen $(\text{CaO})_n\text{Fe}_x\text{O}_y^+$ cluster ions whose structure is closed to those met in the study of calcium chromate [39a] are detected (Fig. 9). These latter lead to a decrease of oxygen amounts available for the formation of highly oxygenated chromium ions and consequently to a reduction of the importance of Cr_2O_6^- ions compared to Cr_2O_4^- ones. With the exception of the Fe_2O_3 – CaCrO_4 mixture, the introduction of significant amounts of trivalent iron and zinc oxides involves a reduction of the R_1 ratio. The limit $R_1 < 0.5$ taken as a criterion to determine if there is any chromium VI or hydrated chromium III compounds is preserved. At the opposite, the $R_1 > 0.8$ limit which indicate the presence of chromium III oxide or chromite compounds does not seem any more a criterion of univocal differentiation. Indeed, the study of

Fe_2O_3 – Cr_2O_3 (respectively, $-\text{ZnCr}_2\text{O}_4$) and ZnO – Cr_2O_3 (respectively, $-\text{FeCr}_2\text{O}_4$) mixtures led to obtaining a R_1 ratio lower than 0.8 (Table 9).

3.3.2. Dependence of the R_1 and R_2 ratio versus the composition of the binary mixtures

Three series of mixtures were examined. They included iron chromite with calcium or silicon oxides in various proportions on the one hand and calcium chromate with various amounts of silica on the other hand. Their compositions are reported in Table 7.

The R_2 ratio is not significantly altered by the introduction of increasing amounts of silica in SiO_2 – CaCrO_4 or SiO_2 – FeCr_2O_4 mixtures. It is systematically characteristic of an anhydrous compound, no significant development is observed versus the portion

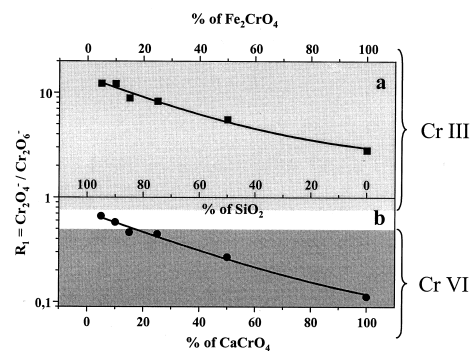


Fig. 10. Development of the R_1 ratio vs. the amounts of silica in the study of binary mixtures including (a) iron chromite (squares) or (b) calcium chromate (circles).

of silica in these two kinds of mixtures. At the opposite, the development of the R_1 ratio is strongly correlated with the amounts of silica in the mixtures (Fig. 10). As described previously, silicon oxide induces less Cr_2O_6^- ions to the benefit of Cr_2O_4^- ones and consequently leads to an increase of the R_1 ratio. This behavior more pronounced when the amounts of silica increase. In fact, the influence of the silicon oxide on this ratio for the iron chromite and the calcium chromate compounds follows an exponential decay and tend to be negligible when the major compound in the mixture studied is FeCr_2O_4 or CaCrO_4 , respectively. The results obtained in the study of the various FeCr_2O_4 – CaO mixtures (not shown) lead to the same behaviors and conclusions.

Finally, the significant correlation between the development of the R_1 ratio and the amounts of calcium or silicon oxides gives some structural information. On the one hand, the results confirm the direct influence of silica (respectively, calcium oxide) on the formation of $\text{Cr}_2\text{O}_{4-6}^-$ cluster ions, in particular by inducing competitive processes that limit the formation of the Cr_2O_6^- ions. On the other hand, the strong dependence of R_1 intensity ratio and the amounts of the oxides free of chromium in the mixtures may be used in the case of simple binary mixture to give quantitative information on the composition of a sample examined.

4. Conclusion

The study of 19 chromium standard compounds with a given FTICRMS analytical sequence allowed us to define criteria of differentiation for hexavalent, trivalent, and hydrated trivalent chromium compounds at $\lambda = 355$ nm with an irradiance of 5×10^7 W/cm^2 . This method, based on the calculation of only two intensity ratios in negative detection mode, ensures the speciation without ambiguity of the +III and +VI chromium chemical states. The confrontation of this methodology to the analysis of chromium compounds mixed with calcium, silicon, trivalent iron, and zinc oxides allows to highlight and to understand the modifications of the mass and to investigate matrix effects. Representing the various processes of

recombination that take place in the gas cloud after the laser ablation/ionization. These modifications show the antagonistic actions in the formation processes of Cr_xO_y^- ions in presence of calcium and silicon oxides on the one hand and of zinc and trivalent iron oxides on the other hand. If the first ones (CaO , SiO_2) tend to disadvantage the formation of the strongly oxygenated species, the second ones (Fe_2O_3 , ZnO) lead on the contrary to the significant formation of these latter. Consequently, whereas the calcium and silicon oxides disturb only slightly the protocol of speciation established, a simple modification of the limits being required, the introduction of hematite and zincite disturb the methodology of speciation. anhydrous trivalent chromium compounds adopt in this case, a similar behavior to that observed for hexavalent chromium compounds. Further, the study of iron chromite–calcium chromate mixture in a mineral matrix including calcium, silicon, trivalent iron and zinc oxides (not shown) illustrates the fact that the antagonistic effects of silica and lime on the one hand and of hematite and the zincite on the other hand have the tendency to be annihilated. In this case, and on the base of the diagram of trivalent and hexavalent chromium differentiation, it is possible to identify the major chromium valence present in these reconstituted matrices.

Moreover, the results obtained in the study of the binary mixtures are interesting from an other point of view. It would be possible to model with the laser ablation/ionization technique, the processes of formation for the oxygenated chromium species, at high temperature in aerosols or dust particles. The microplasma resulting from the laser ablation would be then considered as a chemical microreactor. The proportion dependence of various oxides (CaO , SiO_2 , Fe_2O_3 , ZnO , ...) in the study of chromium compounds on the nature of the species formed would be used to limit the formation of hexavalent chromium species in industrial productions involving chromium species.

Acknowledgement

The authors gratefully acknowledge financial support from Ugine Savoie.

References

- [1] G. Plog, L. Wiedmann, A. Benninghoven, *Surf. Sci.* 67 (1977) 565.
- [2] E. Michiels, R. Gijbels, *Spectrochim. Acta B* 38 (1983) 1347.
- [3] E. Michiels, R. Gijbels, *Anal. Chem.* 56 (1984) 1115.
- [4] F.J. Bruynseels, R.E. Van Grieken, *Anal. Chem.* 56 (1984) 871.
- [5] K.W.M. Siu, G.J. Gardner, S.S. Berman, *Rapid Commun. Mass Spectrom.* 2 (1988) 201.
- [6] I.I. Stewart, G. Horlick, *J. Anal. At. Spectrom.* 11 (1997) 1203, and references therein.
- [7] L. Charles, D. Pepin, B. Casetta, *Anal. Chem.* 68 (1996) 2554.
- [8] L. Charles, D. Pepin, *Anal. Chem.* 70 (1998) 353.
- [9] N. Chaoui, A. Hachimi, E. Millon, J.F. Muller, *Analisis* 24 (1996) 146.
- [10] T.M. Allen, D.Z. Bezabeh, C.H. Smith, E.M. McCauley, A.D. Jones, D.P.Y. Chang, I.M. Kennedy, P.B. Kelly, *Anal. Chem.* 68 (1996) 4052.
- [11] N. Lobstein, E. Millon, A. Hachimi, J.F. Muller, M. Alnot, J.J. Ehrhardt, *Appl. Surf. Sci.* 89 (1995) 307.
- [12] L. Cossarutto, N. Chaoui, E. Millon, J.F. Muller, L. Lambert, M. Alnot, *Appl. Surf. Sci.* 126 (1998) 352.
- [13] S. Colin, G. Krier, H. Jolibois, A. Hachimi, J.F. Muller, A. Chambaudet, *Appl. Surf. Sci.* 125 (1997) 29.
- [14] F. De Smet, M. Devillers, C. Poleunis, P. Bertrand, *J. Chem. Soc., Faraday Trans.* 94 (1998) 941.
- [15] A. Hachimi, P. Shirali, G. Krier, J.F. Muller, J.M. Haguenoer, *Toxicol. Environ. Chem.* 49 (1995) 13.
- [16] A. Hachimi, P. Shirali, G. Krier, M. Brighli, J.F. Muller, J.M. Haguenoer, *J. Mass Spectrom.* (1995) S183.
- [17] B. Maunit, Ph.D. thesis, University of Metz, 1996.
- [18] S. De Nollin, K. Poels, L. Van Vaeck, N. De Clerck, A. Bakker, V. Duwel, D. Vandeveldel, E. Van Marck, *Pathol. Res. Pract.* 193 (1997) 313.
- [19] I.G. Dance, K.J. Fisher, G.D. Willet, *J. Chem. Soc., Dalton Trans.* (1997) 2557.
- [20] E. Poitevin, J.F. Muller, F. Klein, O. Déchelette, *Analisis* 17 (1989) P47.
- [21] A. Hachimi, E. Poitevin, G. Krier, J.F. Muller, M.F. Ruiz-Lopez, *Int. J. Mass Spectrom. Ion Processes* 144 (1995) 23.
- [22] E. Poitevin, G. Krier, J.F. Muller, R. Kaufmann, *Analisis* 20 (1992) M36.
- [23] A. Hachimi, E. Poitevin, G. Krier, J.F. Muller, J. Pironon, F. Klein, *Analisis* 21 (1993) 77.
- [24] K. Poels, L. Van Vaeck, R. Gijbels, *Anal. Chem.* 70 (1998) 504.
- [25] K.R. Neubauer, M.V. Johnston, A.S. Wexler, *Int. J. Mass Spectrom. Ion Processes* 151 (1995) 77.
- [26] A.B. Gwizdala III, S.K. Johnson, S. Mollah, R.S. Houk, *J. Anal. At. Spectrom.* 12 (1997) 503.
- [27] C.J. Cassady, D.A. Weil, S.W. McElvany, *J. Chem. Phys.* 96 (1) (1992) 691.
- [28] B. Maunit, A. Hachimi, P.J. Calba, G. Krier, J.F. Muller, *Rapid Commun. Mass Spectrom.* 9 (1995) 225.
- [29] B. Maunit, A. Hachimi, P. Manuelli, P.J. Calba, J.F. Muller, *Int. J. Mass Spectrom. Ion Processes* 156 (1996) 173.
- [30] A. Thierry de Ville d'Avray, E.E. Carpenter, C.J. O'Connor, R.B. Cole, *Eur. Mass Spectrom.* 4 (1998) 441.
- [31] J. Dennemont, J.C. Landry, *Microbeam Analysis*, p. 305, San Francisco Press, San Francisco, 1985.
- [32] F.J. Bruynseels, R.E. Van Grieken, *Anal. Chem.* 56 (1984) 871.
- [33] F.J. Bruynseels, P. Otten, R.E. Van Grieken, *J. Anal. At. Spectrom.* 3 (1988) 237.
- [34] H. Struyf, L. Van Vaeck, R.E. Van Grieken, *Rapid Commun. Mass Spectrom.* 10 (1996) 551.
- [35] H. Struyf, L. Van Vaeck, K. Poels, R.E. Van Grieken, *J. Am. Soc. Mass Spectrom.* 9 (1998) 482.
- [36] L. Van Vaeck, A. Adriaens, F. Adams, *Spectrochim. Acta B* 53 (1998) 367.
- [37] E. Cuynen, L. Van Vaeck, P. Van Espen, *Rapid Commun. Mass Spectrom.* 130 (1999) 2287.
- [38] M.C. Oliveira, J. Marçalo, M.C. Vieira, M.A. Almoester Ferreira, *Int. J. Mass Spectrom.* 185/186/197 (1999) 825.
- [39] (a) F. Aubriet, B. Maunit, J.F. Muller, *Int. J. Mass Spectrom.* 198 (2000) 189; (b) F. Aubriet, B. Maunit, J.F. Muller, *ibid.* 198 (2000) 213.
- [40] S. Sundar Manoharan, N.R.S. Kumar, K.C. Patil, *MRS Bull.* 25 (1990) 731.
- [41] *Nouveau Traité de Chimie Minérale*, Tome XIV, Masson, Paris, 1957.
- [42] J.F. Muller, M. Pelletier, G. Krier, D. Weil, J. Campana, *Microbeam Analysis—1989*, P.E. Russell (Ed.), San Francisco Press, San Francisco, 1989.
- [43] M. Pelletier, G. Krier, J.F. Muller, D. Weil, M. Johnston, *Rapid Commun. Mass Spectrom.* 2 (1988) 146.
- [44] I.J. Amster, *J. Mass Spectrom.* 31 (1996) 1325.
- [45] F. Aubriet, B. Maunit, B. Courier, J.F. Muller, *Rapid Commun. Mass Spectrom.* 11 (1997) 1596.
- [46] A. Hachimi, E. Millon, E. Poitevin, J.F. Muller, *Analisis* 21 (1993) 11.
- [47] F. Aubriet, Ph.D. thesis, University of Metz, 1999.
- [48] CrO^- : P.G. Wenthold, R.F. Gunion, W.C. Lineberger, *Chem. Phys. Lett.* 101 (1996) 258; CrO_2^- : P.G. Wenthold, K.L. Jonas, W.C. Lineberger, *J. Chem. Phys.* 106 (1997) 9961; CrO_3^- : E.B. Rudnyi, O.M. Vovk, E.A. Kaibicheva, L.N. Sidorov, *J. Chem. Thermodyn.* 21 (1989) 247.
- [49] P.E. Lafargue, J.J. Gaumet, J.F. Muller, A. Labrosse, *J. Mass Spectrom.* 31 (1996) 623.
- [50] S.W. Buckner, J.R. Gord, B.S. Freiser, *J. Chem. Phys.* 88 (1988) 3678.
- [51] <http://webbook.nist.gov/chemistry>.